Geomechanics and Engineering, *Vol. 38, No. 5 (2024) 529-539*
https://doi.org/10.12989/gae.2024.38.5.529

Lifespan assessment of piezoelectric sensors under disposal condition of high-level nuclear waste repository

Changhee Park[1a], Hyun-Joong Hwang[1b], Chang-Ho Hong[2c], Jin-Seop Kim[2d] and Gye-Chun Cho*[1]

[1]*Department of Civil and Environmental Engineering, Korea Advanced Institute of Science and Technology, 291 Daehak-ro, Yuseong-gu, Daejeon 34141, Republic of Korea*
[2]*Disposal Performance Demonstration R&D Division, Korea Atomic Energy Research Institute, 111 Daedeok-daero 989beon-gil, Yuseong-gu, Daejeon, 34057, Republic of Korea*

(*Received November 22, 2023, Revised January 24, 2024, Accepted February 2, 2024*)

Abstract. A high-level nuclear waste (HLW) repository is designed for the long-term disposal of high-level waste. Positioned at depths of 500-1000 meters, it offers an alternative to the insufficient storage space for spent fuels, providing a long-term solution. High-level waste emits heat and radiation, causing structural deterioration, including strength reduction and cracks. Therefore, the use of piezoelectric sensors for structural health monitoring is essential for evaluating the safety of the structure over time. Unlike other structures, the HLW repository restricts human access after the disposal of HLW, rendering sensor replacement impossible. Therefore, it is necessary to assess both the lifespan and suitability of sensors under the disposal conditions in the HLW repository. This study employed an accelerated life test (ALT) to assess the sensor's lifespan under disposal conditions. Failure modes, failure mechanisms, and operational limits were analyzed through accelerated stress test (AST). Additionally, the parameters of the Weibull life probability distribution and the Arrhenius accelerated life model were estimated through statistical methods, including the likelihood ratio test, maximum likelihood estimation, and hypothesis testing. Results confirmed that the sensor's lifespan decreases significantly with the increase in the temperature limit of the HLW repository. The findings of this study can be used for improving sensor lifespan through shielding, development of alternative sensors, or lifespan evaluation of alternative monitoring sensors.

Keywords: accelerated life test; accelerated stress test; high-level nuclear waste; life assessment; piezoelectric sensor

1. Introduction

Spent fuels, a by-product of nuclear power generation, contain high levels of heat and radiation, which pose potential risk to the human living environment. Spent fuels are stored in and managed by either dry or reservoir storage facilities (Kook *et al*. 2013). Data from the third quarter of 2021 reveals that approximately 75% of Korea's overall spent fuel storage capacity has already been utilized. Furthermore, projections suggest that by 2044, 94% of storage capacity will be filled (MOTIE 2021). To mitigate storage scarcity, various disposal methods have been explored, including deep geological, deep-sea, space, and glacier disposals (McKinley *et al*. 2007). The most practical and economically viable solution is a high-level nuclear waste (HLW) repository for deep geological disposal at depths ranging from 500 m to 1000 m (Sjöberg 2004, Kim *et al*. 2011).

The HLW repository comprises a natural barrier system (NBS) composed of bedrock and an engineered barrier system (EBS) designed to complement the nonhomogeneous rock structure, as shown in Fig. 1. An EBS consists of copper canisters, bentonite buffers, disposal tunnels, and backfill materials. Its primary function is to prevent and delay the release of radionuclides by acting as a barrier.

Heat and radiation from nuclear waste can cause structural deterioration of HLW repositories (Jonsson 2012, Kwon *et al*. 2013). Therefore, the disposal volume per unit area is restricted to regulate temperature and radiation. The highest acceptable radiation is 1 Gy/h (Choi *et al*. 2008). The temperature limit for the bentonite buffer material is below 100°C due to the mineralogical transformation and corrosion of bentonite buffer by sediment resulting from the evaporation of groundwater (Rodríguez 2014). Various research groups are working on increasing the temperature limit to improve disposal efficiency and exclude the effects of water or humidity on the structure (Zheng *et al.* 2015, Gens *et al*. 2020). Kim *et al*. (2019) state the effect on bentonite buffer to be insignificant below 150°C. Furthermore, an international collaborative research project, high temperature effects on bentonite buffers (HoTBENT), is investigating the behavior and safety of structures under high-temperature disposal conditions (Kober *et al*. 2023).

The harsh disposal conditions of HLW repositories make structural health monitoring imperative. Specifically, various piezoelectric sensors such as accelerometers, AE and ultrasonic sensors can be used to monitor factors,

*Corresponding author, Professor
E-mail: gyechun@kaist.edu
[a]Master's Student
[b]Ph.D. Candidate
[c]Senior Researcher
[d]Principal Researcher

ISSN: 2005-307X (Print), 2092-6219 (Online)

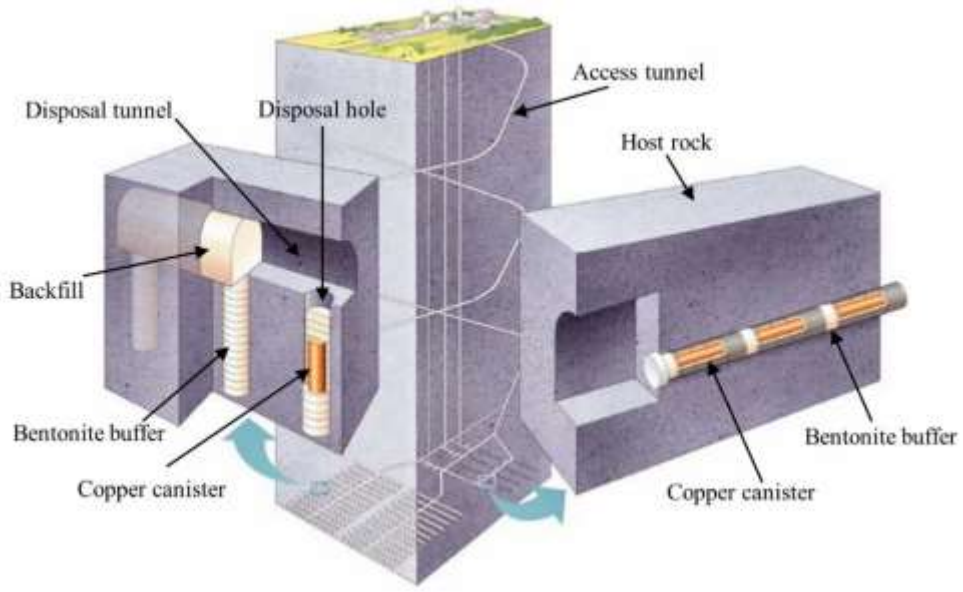

Fig. 1 Schematic of KBS-3 (Nuclear Fuel Safety 3) repository (SKB 2010)

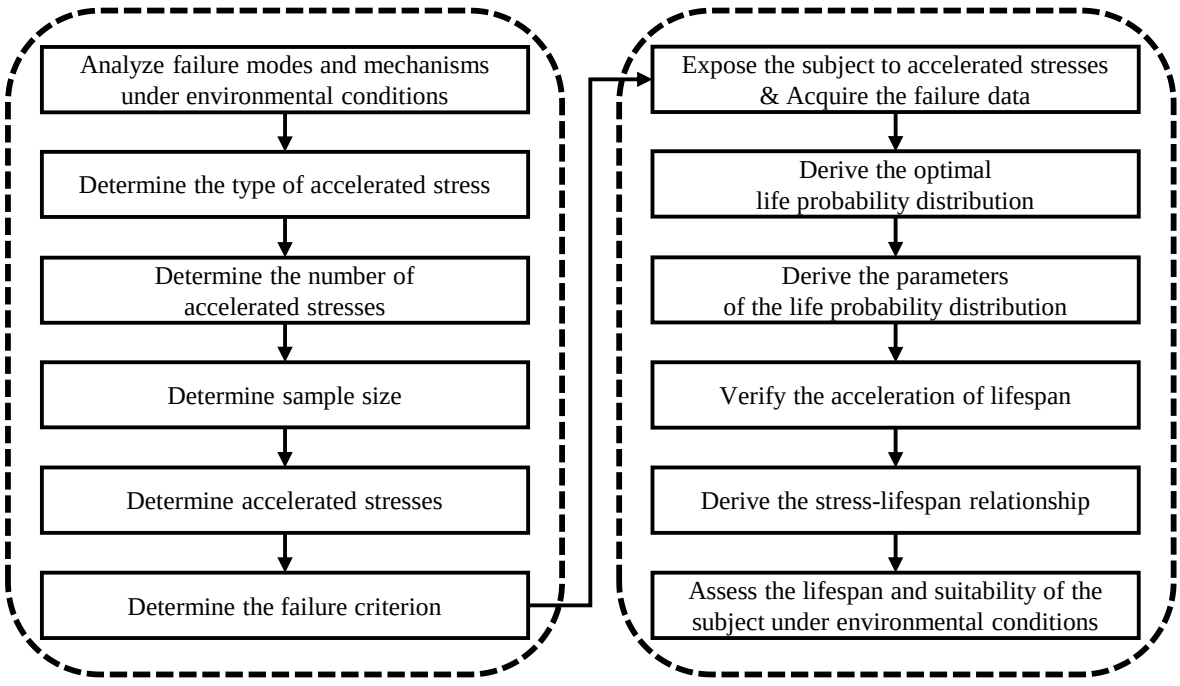

(a) Test design (b) Test analysis

Fig. 2 General process of accelerated life test

including structure strength reduction and cracks. To prevent the leakage of radionuclides, the disposal tunnel is backfilled after nuclear waste disposal, which restricts human access and makes it impossible to replace or remove sensors (Choi *et al*. 2006). Therefore, it is essential to analyze the impact of high temperatures and radiation on piezoelectric sensors and evaluate their suitability through a quantitative lifespan assessment. Exposing the sensors to disposal conditions and observing their failure is the most accurate quantitative method for assessing sensor lifespan. However, this approach is time consuming and expensive. To mitigate this, we employed the accelerated life test (ALT). This method assesses lifespan by exposing accelerated stresses, harsher than the disposal conditions, to induce failure in a shorter period of time (Chernoff 1962, Trevisanello *et al*. 2008). Reliability analysis such as ALT allows one to more specifically treat uncertainties (Goh *et al.* 2010, Hamrouni *et al.* 2018). Ji and Liao (2014), Ghasemi and Nowak (2018), and Dong *et al.* (2022) have recently conducted reliability analyses on slopes, tunnels, and piles, respectively.

The general procedure for the accelerated life test is illustrated in Fig. 2. Initially, the objective is to determine the failure modes that manifest under the disposal

Table 1 Properties of 603C01 related to temperature

Property	Housing	Mass	Electronics	Piezo element
Melting point [°C]	1400~1500	1800~2000	3400~3420	170~180
Thermal conductivity [W/(m·K)]	14~19	130	53~63	1.2~2.3
Thermal expansion coefficient [10^{-6}/°C]	16.8~17.3	7~9	4.4~4.6	3.0~3.5

Table 2 Specification of 603C01

Sensitivity [mV/m/s^2]	981 (±10 %)
Measurement range [m/s^2]	±5.1
Output range [V]	±5
Frequency range [Hz]	0.5~10,000
Resonant frequency [Hz]	25,000

conditions in which the subject is used. The specific disposal conditions that significantly impact the lifespan are identified and selected as stresses for the test. The number of accelerated stresses is generally two or three, and the sample size per accelerated stress is five (Escobar and Meeker 1995, Kim *et al.* 2020). When determining the accelerated stresses, it is crucial to establish levels that replicate the failure modes observed under disposal conditions. This approach ensures highly reliable results. Accelerated stresses should be lower than the operational limit, which causes failure modes different from those in disposal conditions. Once the accelerated stresses are established, the subject is exposed to each stress condition to obtain the corresponding failure data. The collected failure data is used to estimate the relationship between stress and lifespan. This estimation facilitates the assessment of lifespan under the subject's disposal conditions.

This study aimed to assess the lifespan of monitoring piezoelectric sensor in heat and radiation, the main disposal conditions in the HLW repository. We analyzed the failure modes and operational limits of piezoelectric sensors. Based on this analysis, we designed an ALT and used it to assess the lifespan of the piezoelectric sensors. The methodology and results of this study will contribute to future research on the lifespan assessment of various monitoring sensors.

2. Accelerated life test apparatus and methods

We conducted an accelerated stress test (AST) to determine accelerated stresses for ALT, with a focus on understanding failure modes, failure mechanisms, and operational limits. The failure data was collected under the accelerated stresses.

2.1 Test apparatus

In this study, the 603C01 accelerometer from PCB PIEZOTRONICS was selected as the subject for the accelerated life test. This sensor is one of the most widely used piezoelectric sensors in the industry; its schematic is illustrated in Fig. 3, with properties and specification

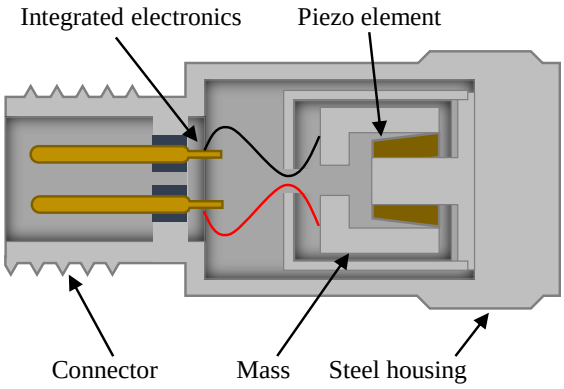

Fig. 3 Schematic of industrial accelerometer

detailed in Tables 1 and 2.

The test was configured to receive signals for determining functional status of the sensor, as shown in Fig. 4. Granite with dimensions of 30 cm × 15 cm × 15 cm was used as the medium to simulate the nature barrier system of the HLW repository. The sensor was attached to the granite specimen using vacuum grease, and a steel ball was dropped from a height of 30 cm on the opposite side to apply a controlled impact to the center of the specimen. The signals generated by the impact were amplified tenfold using a signal conditioner to enhance clarity of collected data. Given the sensor's maximum acquisition frequency of 10 kHz, a low-pass filter set at 10 kHz was applied through a signal filter to reduce noise. Signals were collected using an oscilloscope.

To apply temperature stress to the sensor, we used a Jeiotech OF-22G oven, which is adjustable up to 250°C. For radiation stress, we used a high-level gamma-ray irradiator facility at the Korea Atomic Energy Research Institute's Jeongeup branch. The irradiator, emitted gamma rays of Cobalt-60 with a controllable dose rate ranging from 10 kGy/h (Fig. 5).

2.2 Failure mode

Piezoelectric sensors operate based on the piezoelectric effect; they convert mechanical stress into electrical charge. When impacted, the piezoelectric element in these sensors vibrates, translating these vibrations into electrical signals. These sensors may experience failures under high-temperature or radiation conditions. Under high-temperature conditions, failure modes include altered signal sensitivity from deformation of the piezo element or signal interruption caused by the destruction of the piezo element

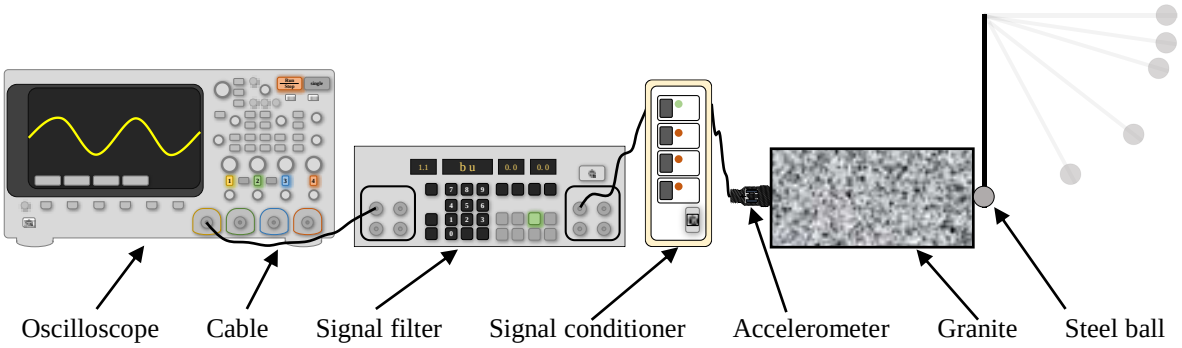

Fig. 4 Test setup

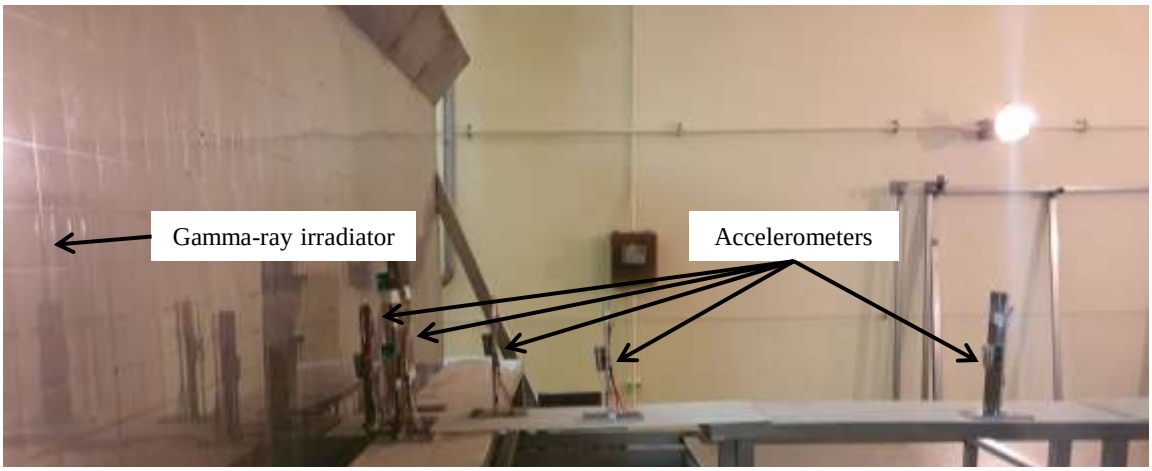

Fig. 5 High-level gamma-ray irradiator facility

(Wlodkowski 1999, Marozau *et al*. 2018). In high-level radiation conditions, the failure mode of piezoelectric sensors primarily results from non-ionizing energy loss (NIEL). This involves atomic displacements caused by radiation energy, which reduce the activity of electrons (Shea 2009).

We conducted experiments to confirm the failure modes and mechanisms under various disposal conditions. The presence of failures was determined by comparing the difference between the signal in the normal state and that under harsh conditions. Signals were collected in both time and frequency domains. In the time domain, measurements included the peak value representing a single amplitude of the signal and the peak-to-peak value representing double the amplitude of the signal. In the frequency domain, measurements included the resonant frequency, indicative of the natural frequency that causes significant oscillations. According to industry standards operational fluctuations in the signal sensitivity of piezoelectric sensors within a range of ±20% are considered normal (Hwang *et al*. 2022). Therefore, in this study, we defined a failure as any deviation of the sensor's signal beyond ±20% from the signal acquired under normal conditions.

Since the maximum adjustable temperature limit of the HLW repository was 150℃, we simulated temperature conditions of 140℃ using an oven, and exposed five sensors to it. We collected five impact signals every 24 hours and determined failures based on the average value.

Table 3 Experimental cases for failure modes

Stress type	temperature stress	radiation stress
Stress level	140℃	1, 3, 5, 7, 9kGy/h
Sample size	5	2 for each stress
Exposure time [hours]	480~1008	103

Table 4 Results: the number of failed samples & failure modes under the disposal conditions

Property	temperature stress	radiation stress
The number of failed samples	2	0 of 10
Failure time [hours]	480, 864	N/A
Failure mode	change in signal sensitivity	N/A

The experiment was conducted for 1008 hours, and the sensors that experienced failures were removed from the measurements.

Due to the dose rate control limitations of the gamma radiation facility, simulating the disposal conditions with a dose rate of 1 Gy/h was impossible. Instead, we simulated radiation conditions with dose rates of 1, 3, 5, 7, and 9 kGy/h. The two sensors were exposed to each condition. In addition, the complex operational procedures of the

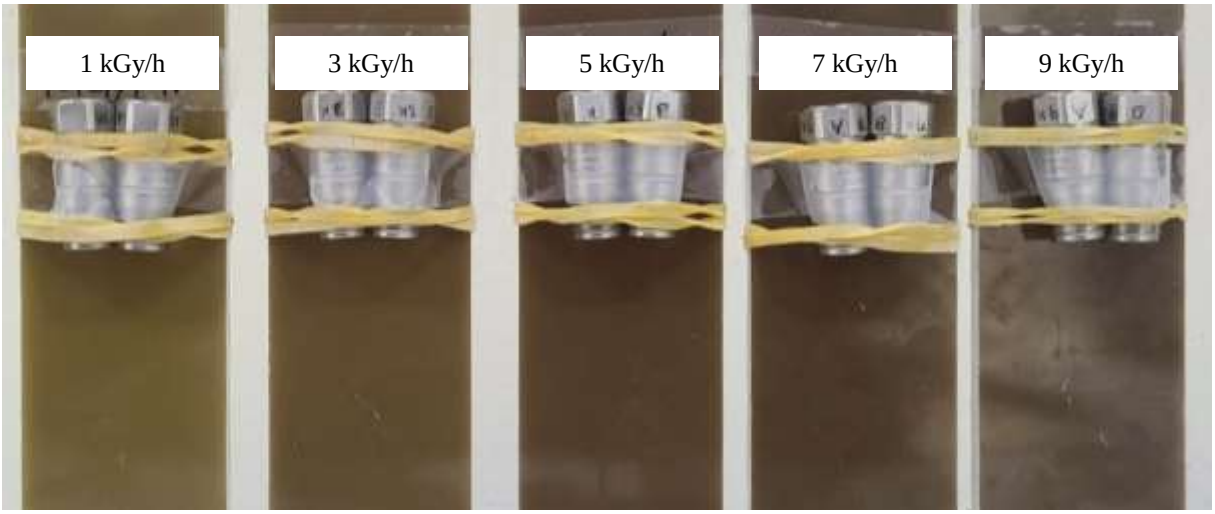

Fig. 6 Accelerometers exposed to radiation stress

irradiation facility meant that signals could not be collected at regular intervals. Therefore, we collected five impact signals when the facility was temporarily stopped and determined failures based on the average value. The experiment lasted 103 hours, and the sensors that experienced failures were removed from the measurement.

The experimental cases for the failure modes are listed in Table 3, and the results are presented in Table 4. Under the temperature conditions of the HLW repository, the predominant failure mode observed was a change in signal sensitivity. The recognized failure mode also endured at room temperature once it was identified as a failure. In contrast, under radiation conditions, although the rubber band's corrosion and plate's external change were observed (Fig. 6), no sensor failures occurred during the signal collection process. We applied a cumulative radiation dose of 927 kGy based on the maximum experimental condition of 9 kGy/h. This dose is equivalent to the exposure that would occur over 105.8 years in the HLW repository, under the radiation dose limit of 1 Gy/h. Woo (2018) states that general monitoring sensors have a service lifespan of 9 to 10 years. Given this, we conclude that the radiation conditions in the HLW repository do not significantly affect sensor lifespan.

2.3 Operational limit

The AST is used to identify the operational limit, that is, the stress level at which unexpected failure modes occur. AST is carried out by subjecting the sensor to gradually increasing or incremental stress. ALT requires determining accelerated stresses that induce the same failure modes as those that occur under disposal conditions (Kim and Bai 2002). Therefore, these stresses should be set lower than the operational limit derived through the AST.

As the previous subsection confirmed that radiation stress does not have a significant effect on lifespan, AST was performed only for the temperature stress. Failure was determined by comparing the difference between the signal in the normal state and that under disposal conditions.

Table 5 Experimental cases for AST

Stress type	temperature stress
Stress level [℃]	130 ~180
Sample size	5
Exposure time [hours]	8 for each stress

Table 6 Results: the number of failed samples & failure modes under the operational limit

Stress level [℃]	The number of failed samples	Failure time [hours]	Failure mode
130	0	N/A	N/A
140	0	N/A	N/A
150	0	N/A	N/A
160	0	N/A	N/A
170	0	N/A	N/A
180	5	1 for all failures	signal interruption

Measurements in the time domain included peak and peak-to-peak values, and the resonant frequency was measured in the frequency domain.

AST was conducted starting from 130℃, which is below 140℃ with a predictable failure mode according to results of subsection 2.2. The temperature was then gradually increased in increments of 10℃ until the operational limit was reached. The two sensors were exposed to temperature stresses, and five impact signals were collected every hour to determine failures based on the average value. If no failure occurred within 8 hours, the sensors were exposed to 25℃ for 16 hours, followed by exposure to temperature stress incremented by 10℃. This process was repeated until the operational limit was reached.

Experimental cases for the AST are detailed in Table 5, and the results are presented in Table 6. Under the high-temperature disposal conditions of the HLW repository, failure mode was identified as a change in signal sensitivity.



(a) Normal state at 20℃ (b) Piezo element deformation at 140℃ (c) Piezo element destruction at 180℃

Fig. 7 Failure mechanism at different temperatures

Table 7 Experimental cases for failure mechanism

Stress type	temperature stress		
Stress level [℃]	20	140	180
Sample size	2	2	2
Exposure time [hours]	24	24	24

Table 8 Experimental cases for ALT

Stress type	temperature stress		
Stress level [℃]	150	160	170
Sample size	5	5	5
Exposure time [hours]	840~2976	240~744	28~88

However, at 180℃, the initial measurement revealed a failure mode of signal interruption, which differed from the failure mode observed under disposal conditions. This suggested that the operational limit was 180℃. Therefore, it was reasonable to set the accelerated stresses lower than 180℃, such as 170, 160, and 150℃.

2.4 Failure mechanism

Subsections 2.2 and 2.3 outline the failure modes of signal sensitivity change at 140℃, which represents the disposal condition of the HLW repository, and the signal interruption at the operational limit of 180℃. We conducted an experiment to verify whether the failure mechanisms causing the two failure modes, as identified in previous studies, were the deformation and destruction of the piezo elements. Each of the two piezo elements were exposed to the temperatures 140 and 180℃, simulated using ovens. Following 24-hour exposure, we collected five impact signals using to determine failures based on their average value. Experimental cases for the failure mechanisms are listed in Table 7, and the results are presented in Fig. 7. As anticipated, the experiment confirmed the failure mechanisms: deformation of piezo elements at 140℃ and destruction of piezo elements at 180℃. These results are consistent with the previously conducted ASTs, affirming that the accelerated stresses at 170, 160, and 150℃ are reasonable.

Table 9 Statistics of life probability distributions

Distribution	AIC	-2Loglikelihood	BIC
Weibull	205.78	198.23	206.36
Loglogistic	206.41	198.55	206.67
Fréchet	207.52	199.34	207.46
Exponential	211.32	206.32	211.73
LEV (Largest Extreme Value)	230.82	222.64	230.76
Logistic	233.44	225.26	233.39
Normal	237.50	229.31	237.44
SEV (Smallest Extreme Value)	243.05	234.87	242.99

2.5 Failure data analysis

Ovens were used to simulate temperatures of 150, 160, and 170℃ with five sensors exposed to each of these conditions. Five impact signals were collected every 2 or 24 hours to determine failures based on the average value. We conducted the ALT until all sensors failed; any sensors that failed were discontinued from the measurement. Experimental cases of the ALT are presented in Table 8. The analysis of the failure data was analyzed using three statistical methods.

First, the acquired failure data were used to determine the optimal probability distribution using a likelihood ratio test. The likelihood ratio test used to evaluate the adequacy of two competing models. It involves comparing the likelihoods of the models, where one is obtained by maximizing across the whole parameter space, and the other is obtained by imposing a specified restriction. The test determines the goodness of fit by examining the ratio of these likelihoods data (D'Agostino 2017).

Subsequently, the probability distribution parameters were obtained through maximum likelihood estimation. Maximum likelihood estimation is used to estimate the parameters of a presumed probability distribution based on observed data (Dennis Jr and Schnabel 1996).

Finally, acceleration of lifespan was verified by hypothesis testing that determines if the available data provides enough support for a specific hypothesis.

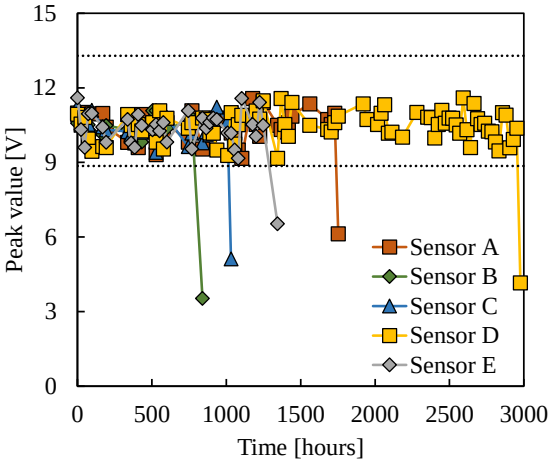

(a) Failure time with peak value

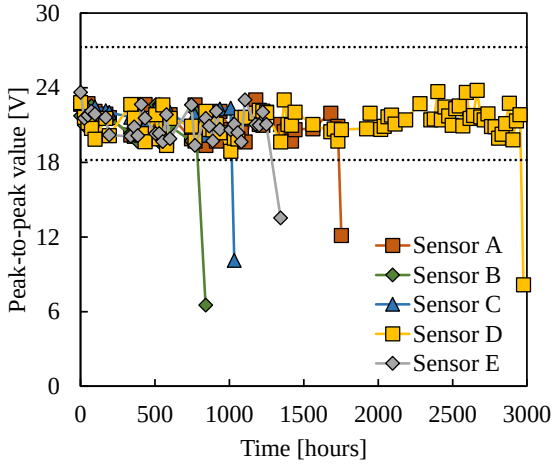

(b) Failure time with peak-to-peak value

Fig. 8 Failure time at 150℃

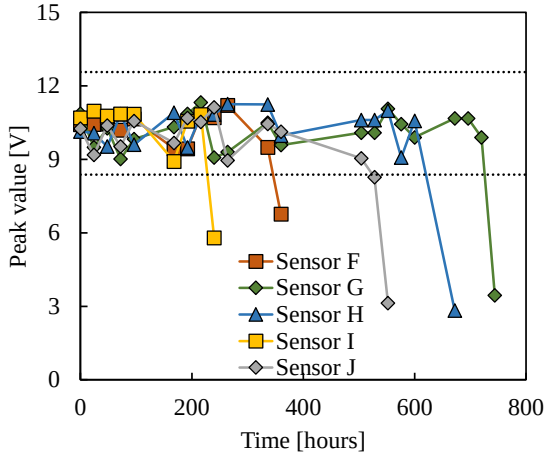

(a) Failure time with peak value

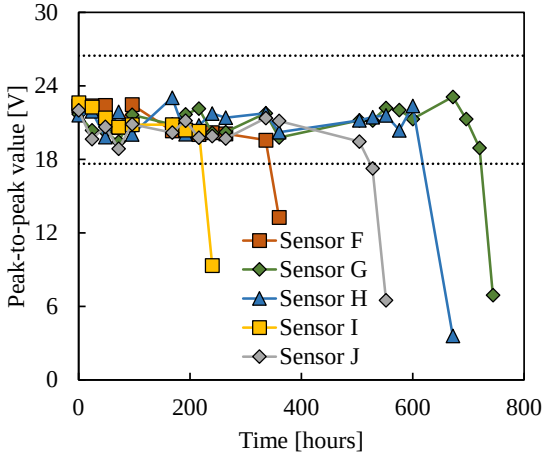

(b) Failure time with peak-to-peak value

Fig. 9 Failure time at 160℃

3. Accelerated life test results and discussion

The failure results under accelerated stresses of 150, 160, and 170℃ in ALT are presented in this section. As anticipated, all sensors exposed to the accelerated stresses showed a failure mode characterized by a change in signal sensitivity, but no alteration was observed in the frequency domain. Therefore, we present only the signal in time domain (Figs. 8-10). Statistical methods such as the likelihood ratio test, maximum likelihood estimation, and hypothesis testing were employed for result analysis.

3.1 Optimal life probability distribution

We applied the likelihood ratio test to obtain the optimal life probability distribution from the failure. Likelihood refers to a value that indicates the probability distribution from which a specific set of data is most likely to have originated. The likelihood ratio test was used to assess the significance of the regression coefficients by comparing the ratio of likelihoods for each distribution. The actual set of failure data is considered the reduced model, whereas the distribution that describes the trend in the data is known as the full model. The parameters of each model are assumed to be β^1 and β^0, respectively. When the likelihood function of the reduced model is L_0, the likelihood function of the full model is L_1, and their respective maximum likelihood estimations are $\hat{\beta}^1$ and $\hat{\beta}^0$. The likelihood ratio test statistic D is expressed as shown in Eq. (1).

$$D = -2\left(L_0(\hat{\beta}^1) - L_1(\hat{\beta}^1)\right) \tag{1}$$

In addition, accounting for the number of parameters and the amount of data, we derive the Akaike Information Criterion (AIC) and Bayesian Information Criterion (BIC) as shown in Eqs. (2) and (3)

$$AIC = -2Loglikelihood + 2K \tag{2}$$

$$BIC = -2Loglikelihood + K\log n \tag{3}$$

where $Loglikelihood = L_0(\hat{\beta}^1) - L_1(\hat{\beta}^1)$, K is the

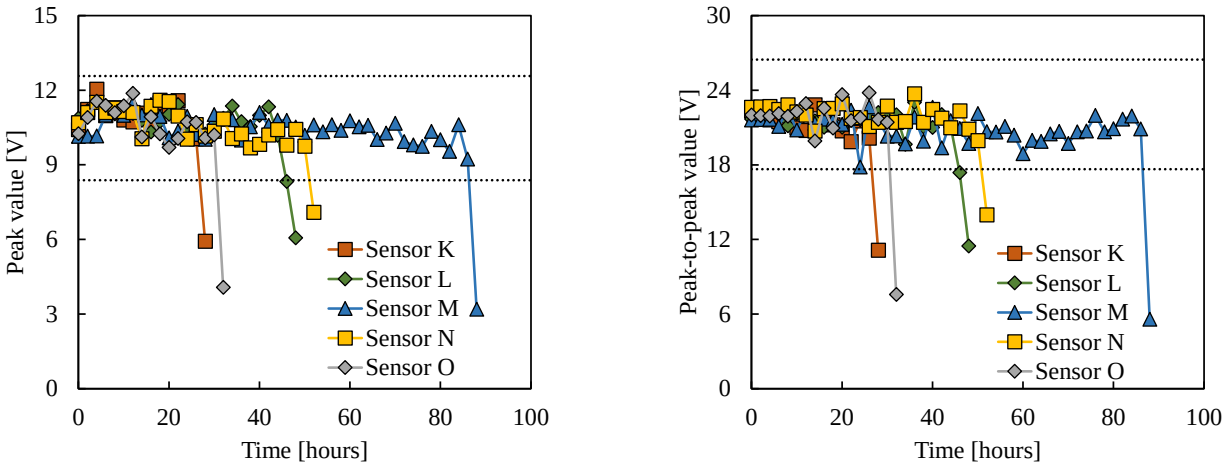

(a) Failure time with peak value (b) Failure time with peak-to-peak value

Fig. 10 Failure time at 170℃

number of parameters in the model, and n is the number of data points.

The likelihood ratio test was conducted using JMP software version 17.0.0. It provides a range of statistical and analytical tools for data analysis, exploration, and visualization (Sall *et al*. 2017). Table 9 presents the likelihood ratio test results. The test results showed that the Weibull life probability distribution, which exhibits the minimum value for all parameters, is the most suitable to describe the collected failure data.

3.2 Parameters of Weibull life probability distribution

Eq. (4) represents the failure rate function of the Weibull life probability distribution, assuming that the failure data are independent.

$$W\sim\lambda(t,T)=\frac{f(t,T)}{R(t,T)}=\frac{\beta(T)}{\eta(T)}\left(\frac{t}{\eta(T)}\right)^{\beta(T)-1} \tag{4}$$

where $\lambda(t,T)$ is the failure rate function, $f(t,T)$ is the failure probability density function, $R(t,T)$ is the reliability function, $\beta(T)$ is the shape parameter, $\eta(T)$ is the scale parameter, t is time, T is the absolute temperature. $R(t,T)$ represents the probability that the system or its components function without failure up to time t. Relationships between $R(t,T)$, $f(t,T)$, And The failure cumulative distribution function $F(t,T)$ are represented by Eqs. (5) and (6)

$$\begin{aligned} f(t,T)&=\frac{dF(t,T)}{dt}=\frac{d\big(1-R(t,T)\big)}{dt}\\ &=\frac{\beta(T)t^{\beta(T)-1}}{\eta(T)^{\beta}}e^{-\left(\frac{t}{\eta(T)}\right)^{\beta(T)}} \end{aligned} \tag{5}$$

$$F(t,T)=\int_0^{\infty}f(t,T)\,dt=1-\exp\left[-\left(\frac{t}{\eta(T)}\right)^{\beta(T)}\right] \tag{6}$$

where $F(t,T)$ is the failure cumulative distribution function.

We used the maximum likelihood estimation method to find the shape and scale parameters of the Weibull life probability distribution. The likelihood function of the distribution was found following Eq. (7), and the logarithmic likelihood function was found using Eq. (8)

$$L\left(\beta,\frac{1}{\eta};t_1,t_2,\dots,t_n\right)=\frac{\beta^n}{\eta^{\beta n}}\prod_{j=1}^{n}t_j^{\beta-1}e^{-\left(\frac{t_j}{\eta}\right)^{\beta}} \tag{7}$$

$$\begin{aligned} l\left(\beta,\frac{1}{\eta}\right)&=\ln L(\beta,\eta;t_1,t_2,\dots,t_n)\\ &=n\ln\beta+n\beta\ln\frac{1}{\eta}+(\beta-1)\sum_{j=1}^{n}\ln t_j-\frac{1}{\eta^{\beta}}\sum_{j=1}^{n}t_j^{\beta} \end{aligned} \tag{8}$$

where n denotes the number of data points. Eqs. (9) and (10) are the results of partially differentiating Eq. (8) with regard to $\frac{1}{\eta}$ and β.

$$\frac{\partial l}{\partial\frac{1}{\eta}}=n\beta\eta-\frac{\beta}{\eta^{\beta-1}}\sum_{j=1}^{n}t_j^{\beta}=0 \tag{9}$$

$$\frac{\partial l}{\partial\beta}=n\beta+n\ln\frac{1}{\eta}+\sum_{j=1}^{n}\ln t_j-\sum_{j=1}^{n}\left(\frac{t_j}{\eta}\right)^{\beta}\ln\frac{t_j}{\eta}=0 \tag{10}$$

The solutions to Eqs. (9) and (10) yield the maximum likelihood estimations, $\hat{\beta}$ and $\hat{\eta}$. From Eq. (9), $\hat{\eta}$ is expressed as Eq. (11).

$$\hat{\eta}=\left(\frac{\sum_{j=1}^{n}t_j^{\hat{\beta}}}{n}\right)^{\frac{1}{\hat{\beta}}} \tag{11}$$

Substituting Eq. (11) into Eq. (10), $\hat{\beta}$ is expressed as Eq. (12).

$$\frac{n}{\hat{\beta}}+\sum_{j=1}^{n}\ln t_j-\frac{n\sum_{j=1}^{n}t_j^{\hat{\beta}}\ln t_j}{\sum_{j=1}^{n}t_j^{\hat{\beta}}}=0 \tag{12}$$

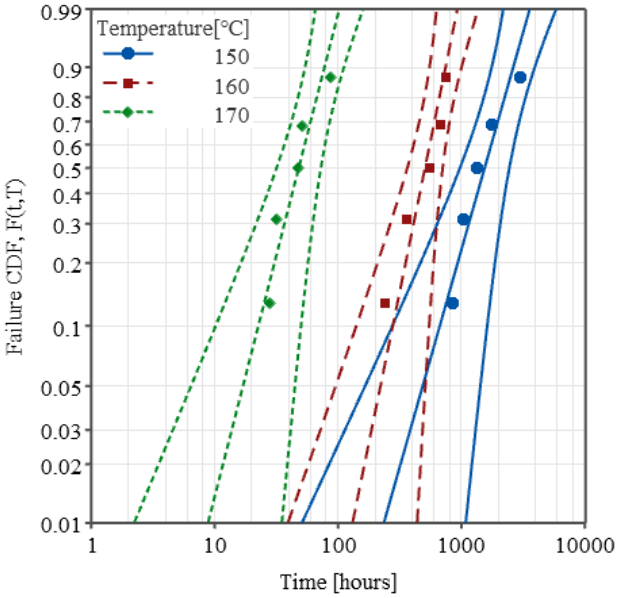

Fig. 11 Failure cumulative distribution function

Table 10 Hypothesis testing conditions

Null hypothesis	H_0: $\beta(150\,°C) = \beta(160\,°C) = \beta(170\,°C) = \beta$
Alternative hypothesis	H_1: At least one of the shape factors is different
Significance level	$\alpha = 0.05$

The solution $\hat{\beta}$ for Eq. (12) was calculated using Minitab software version 21.1.0. Minitab provides a range of statistical tools for analyzing data, making informed decisions, and solving problems (Evans 2009). $\hat{\beta}$ calculated for 150, 160, and 170°C were 2.25, 3.31, and 2.50, respectively. Substituting these values into Eq. (11) yields $\hat{\eta}$ of 1804.70, 576.75, and 56.15, respectively.

The plot of the failure cumulative distribution function $F(t,T)$ on Weibull probability paper with a 95% confidence interval is shown in Fig. 11 by substituting the two parameters into Eq. (6). On the Weibull probability paper, the horizontal axis represents $\ln t$ and the vertical axis represents $\ln[-\ln(1-F(t,T))]$.

3.3 Verification of acceleration

Predict the sensor's lifespan under stress conditions different to accelerated stress, required proving that temperature stress accelerates sensor's lifespan. This implied that all the shape parameters for the accelerated stresses would remain identical. Therefore, a hypothesis testing was conducted, using Minitab, with the null hypothesis assuming that all shape parameters are the same and the alternative hypothesis assuming that at least one of the shape parameters was different Table 10.

The hypothesis testing found the equal shape factor β to be 2.02, and the p-value 0.803. This value greatly exceeded the significance level of 0.05, suggesting that the null hypothesis is likely to be true (Sellke *et al*. 2001). This proved that the sensor lifespan was accelerated by the temperature stress.

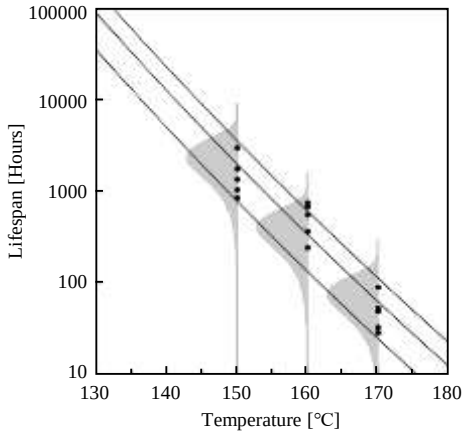

Fig. 12 Lifespan under temperature stress

Table 11 Lifespan under temperature stress

Temperature stress = 130°C	
$F(t,T)$	$F\left(t, 130°C\right) = 1 - \exp\left[-\left(\frac{t}{106175.95}\right)^{2.02}\right]$
L_n	> the service lifespan
B_{10}	34894.8 hours = 3.98 years
Temperature stress = 135°C	
$F(t,T)$	$F\left(t, 135°C\right) = 1 - \exp\left[-\left(\frac{t}{39541.42}\right)^{2.02}\right]$
L_n	39541.42 hours = 4.51 years
B_{10}	12995.31 hours = 1.48 years
Temperature stress = 140°C	
$F(t,T)$	$F\left(t, 140°C\right) = 1 - \exp\left[-\left(\frac{t}{15082.08}\right)^{2.02}\right]$
L_n	15082.08 hours = 1.72 years
B_{10}	4956.74 hours = 0.57 years

3.4 Lifespan of piezoelectric sensors

The previous section has confirmed that physical or chemical alterations occur in the sensor due to temperature stress. Therefore, we used the Arrhenius accelerated life model, which represents the response dependence of the temperature stress, as the ALT (Nelson 2009). The reaction rate and yield due to the temperature stress, according to the Arrhenius-accelerated life model are represented by Eqs. (13) and (14)

$$v_r = \gamma \cdot e^{-\frac{E_a}{k \cdot T}} \tag{13}$$

$$x = v_r t \tag{14}$$

where v_r is the rate constant of the reaction, γ is the frequency factor, E_a is the activation energy of the reaction, k is Boltzmann constant 8.617×10^{-5}, T is the absolute temperature, and x is the reaction yield. For accelerated life tests, when failure occurs, and the reaction yield reaches x_0, the nominal lifespan L_n is expressed in Eq. (15).

$$x_0 = \gamma \cdot e^{-\frac{E_a}{k \cdot T}} \cdot L_n$$

$$L_n = \left(\frac{x_0}{\gamma}\right) \exp\left(\frac{E_a}{k \cdot T}\right) \tag{15}$$

The parameters obtained from the regression analysis using Minitab with $\ln\left(\frac{x_0}{\gamma}\right)$ and E_a are -69.06 and -2.80, respectively. By substituting these parameters into Eq. (15), we express the relationship between the nominal lifespan of the sensor and the temperature stress as detailed in Eq. (16)

$$L_n = 1.02 \times 10^{(-30)} \cdot \exp\left(\frac{32507.83}{T^{'} + 273.15}\right) \quad (16)$$

where $T^{'}$ is temperature in Celsius.

The nominal lifespan L_n, obtained from the Arrhenius-accelerated life model in Eq. (16) represents the 63.2 percentile of the lifespan. This is equivalent to the scale parameter $\eta(T)$ of the Weibull life probability distribution. By substituting this scale parameter for each of the temperatures 150, 160, and 170℃ into Eq. (5), we can plot the Weibull lifespan probability distribution alongside Arrhenius accelerated model, as shown in Fig. 12.

By substituting 9 years, the typical service lifespan of a monitoring sensor into Eq. (16), we calculated the temperature to be 131.50℃. This implies that, in terms of nominal lifespan, temperature stress does not significantly affect the lifespan until it reaches approximately 130℃. However, given the characteristics of the HLW repository, where sensor replacement is not feasible, it is essential to consider a stricter lifespan criterion than the nominal lifespan of the 63.2 percentile lifespan. Assuming the service lifespan is the 10th percentile lifespan B_{10} and substituting it into Eq. (6), the scale parameter was estimated to be 239663.41. By substituting the scale parameter into Eq. (16), the temperature was calculated to be 125.97℃. This suggest that in terms of the 10th percentile lifespan, temperature stress does not significantly affect the lifespan until it reaches approximately 125℃.

Assuming the sensors are exposed to disposal conditions of 130, 135, and 140℃ due to the increased temperature limit of the HLW repository, the nominal lifespan calculated using Eq. (16) can be substituted into Eq. (6) to determine the failure cumulative distribution function, 10th percentile lifespan, and nominal lifespan for each temperature condition, as listed in Table 11.

With each 5℃ increment, the lifespan of the sensors decreases significantly. Given the ongoing discussions about raising the temperature limit in HLW repositories, this clearly indicates that general industrial piezoelectric sensors are unsuitable for such conditions. Therefore, further studies are necessary to explore sensor lifespan enhancements, including options like sensor shielding or the development of alternative sensors.

This study established the correlation between temperature and the lifespan of the piezoelectric sensor through the utilization of three accelerated stress levels. While employing more stress levels could have yielded more enhanced results, the characteristic of ALT, which consumes considerable time, led to the utilization of only three levels. This can be a limitation of the study.

4. Conclusions

In this study, we conducted an accelerated life test to assess the lifespan and suitability of piezoelectric sensors under the disposal conditions of a high-level waste repository. The effects of temperature and radiation stress on lifespan were analyzed experimentally and statistically. The findings of this study provide a framework for testing sensor lifespan in high temperature and radiation conditions of the HLW repository. This framework can be summarized as follows:

- Under the HLW repository temperature conditions, the failure mode of the piezoelectric sensor was the signal sensitivity change, and the failure mechanism was identified as the deformation of the piezoelectric element. However, there was no observed failure of the piezoelectric sensor attributed to radiation.
- The accelerated stress test aimed to establish the temperature stress operational limit, which was determined as 180 °C. Consequently, 150, 160, and 170°C were chosen as accelerated stresses for the ALT.
- The Weibull life probability distribution was identified as the optimal life probability distribution to describe the collected failure data. using the likelihood ratio test.
- The relationship between the shape and scale parameters of the Weibull life probability distribution was estimated using the maximum likelihood estimation. The acceleration of the lifespan due to temperature stress was verified through a hypothesis testing based on the equal shape factor.
- The Arrhenius accelerated model was utilized to represent the physical and chemical deformations caused by the temperature stress. This model was used to derive the relationship between the nominal lifespan and temperature stress. Furthermore, the nominal and 10th percentile lifespans under the disposal conditions of the HLW repository were derived.
- Lifespan significantly decreased with a slight increase in temperature stress. Given the discussion on increasing the temperature limit in HLW repositories, general industrial piezoelectric sensors are concluded unsuitable for these conditions. Hence, further studies are required to investigate methods for extending the lifespan of sensors, including sensor shielding and the development of alternative sensing technologies.

Acknowledgments

This research was supported by the Nuclear Research and Development Program of the National Research Foundation of Korea (2022M2E3A3015608) funded by the Minister of Science and ICT. The first author was supported by the Innovated Talent Education Program for Smart Cities of MOLIT.

References

Chernoff, H. (1962), "Optimal accelerated life designs for estimation", *Technometrics*, **4**(3), 381-408. https://doi.org/10.1080/00401706.1962.10490020.

Choi, H.J., Lee, J.Y. and Kim, S.S. (2008), "Korean reference HLW disposal system", KAERI/TR-3563/2008, Korea Atomic Energy Research Institute.

Choi, J.W., Choi, H.J., Lee, J.Y. and Chun, K.S. (2006), "High-level radwaste disposal technology development", KAERI/RR-2765/2006, Korea Atomic Energy Research Institute.

D'Agostino, R.B. (1986), Goodness-of-Fit-Techniques. Routledge, New York, NY, U.S.A.

Dennis Jr, J.E. and Schnabel, R.B. (1996). Numerical Methods for Unconstrained Optimization and Nonlinear Equations. Society for Industrial and Applied Mathematics. Philadelphia, Commonwealth of Pennsylvania, U.S.A.

Dong, X., Tan, X., Lin, X., Zhang, X., Hou, X. and Wu, D. (2022), "Reliability analysis of piles based on proof vertical static load test", *Geomech. Eng.*, **29**(5), 487-496. https://doi.org/10.12989/gae.2022.29.5.487.

Escobar, L.A. and Meeker, W.Q. (1995), "Planning accelerated life tests with two or more experimental factors", *Technometrics*, **37**(4), 411-427. https://doi.org/10.1080/00401706.1995.10484374.

Evans, M. (2009), Minitab manual. W.H. Freeman and Company, New York, NY, USA.

Gens Solé, A., Barboza de Vasconcelos, R. and Olivella Pastallé, S. (2020), "Towards higher temperatures in nuclear waste repositories", *E3S web of conferences*, **205**(01001), 1-8. https://doi.org/10.1051/e3sconf/202020501001.

Ghasemi, S.H. and Nowak, A.S. (2018), "Reliability analysis of circular tunnel with consideration of the strength limit state", *Geomecha. Eng.*, **15**(3), 879-888. https://doi.org/10.12989/gae.2018.15.3.879.

Goh, A.T. and Hefney, A.M. (2010), "Reliability assessment of EPB tunnel-related settlement", *Geomech. Eng.*, **2**(1), 57-69. https://doi.org/10.12989/gae.2010.2.1.057.

Hamrouni, A., Dias, D. and Sbartai, B. (2018), "Reliability analysis of a mechanically stabilized earth wall using the surface response methodology optimized by a genetic algorithm", *Geomech. Eng.*, **15**(4), 937-945. http://doi.org/10.12989/gae.2018.15.4.000

Hwang, H.J., Park, C., Hong, C.H., Kim, J.S. and Cho, G.C. (2022), "Design of accelerated life test on temperature stress of piezoelectric sensor for monitoring high-level nuclear waste repository", *J. Korean Tunn. Undergr. Sp. Assoc.*, **24**(6), 451-464. https://doi.org/10.9711/KTAJ.2022.24.6.451.

Ji, J. and Liao, H.J. (2014), "Sensitivity-based reliability analysis of earth slopes using finite element method", *Geomech. Eng.*, **6**(6), 545-560. https://doi.org/10.12989/gae.2014.6.6.545.

Jonsson, M. (2012), "Radiation effects on materials used in geological repositories for spent nuclear fuel", *Int. Scholarly Res.Notices*, **2012**. https://doi.org/10.5402/2012/639520.

Kim, C.M. and Bai, D.S. (2002), "Analyses of accelerated life test data under two failure modes", *Int. J. Reliab. Quality Saf. Eng.*, **9**(2), 111-125. https://doi.org/10.1142/S0218539302000706.

Kim, J.S., Cho, W.J., Park, S., Kim, G.Y. and Baik, M.H. (2019), "A review on the design requirement of temperature in high-level nuclear waste disposal system: based on bentonite buffer", *J. Korean Tunn. Undergr. Sp. Assoc.*, **21**(5), 587-609. https://doi.org/10.9711/KTAJ.2019.21.5.587.

Kim, J.S., Kwon, S.K., Sanchez, M. and Cho, G.C. (2011), "Geological storage of high level nuclear waste", *KSCE J. Civil Eng.*, **15**(4), 721-737. http://doi.org/10.1007/s12205-011-0012-8.

Kim, S.H., Yeom, J., Baek, I.S., Kim, J.S. and Sung, S.I. (2020), "Determining the statistical sample size for reliability testing", *J. Appl. Reliab.*, **20**(1), 84-93. https://doi.org/10.33162/JAR.2020.3.20.1.84.

Kober, F., Schneeberger, R., Vomvoris, S., Finsterle, S. and Lanyon, B. (2023), "The HotBENT Experiment: objectives, design, emplacement and early transient evolution", *Geoenergy*, **1**(1), 2023-021. https://doi.org/10.1144/geoenergy2023-021.

Kook, D., Choi, J., Kim, J. and Kim, Y. (2013), "Review of spent fuel integrity evaluation for dry storage", *Nuclear Eng. Tech.*, **45**(1), 115-124. https://doi.org/10.5516/NET.06.2012.016.

Kwon, S., Cho, W.J. and Lee, J.O. (2013), "An analysis of the thermal and mechanical behavior of engineered barriers in a high-level radioactive waste repository", *Nuclear Eng. Tech.*, **45**(1), 41-52. https://doi.org/10.5516/NET.06.2012.015.

Marozau, I., Auchlin, M., Pejchal, V., Souchon, F., Vogel, D., Lahti, M. and Sereda, O. (2018), "Reliability assessment and failure mode analysis of MEMS accelerometers for space applications", *Microelectron. Reliab.*, **88**, 846-854. https://doi.org/10.1016/j.microrel.2018.07.118.

McKinley, I.G., Alexander, W.R. and Blaser, P.C. (2007), "Development of geological disposal concepts", *Radioactivity in the Environment*, **9**, 41-76. https://doi.org/10.1016/S1569-4860(06)09003-6

MOTIE (2021), "A second basic national plan for HLW management", Ministry of Trade, Industry and Energy.

Nelson, W.B. (2009), Accelerated testing: statistical models, test plans, and data analysis, John Wiley & Sons, Hoboken, State of New Jersey, U.S.A.

Rodríguez, M.A. (2014), "Anticipated degradation modes of metallic engineered barriers for high-level nuclear waste repositories", *JOM*, **66**(3), 503-525. http://doi.org/10.1007/s11837-014-0873-7

Sall, J., Stephens, M.L., Lehman, A. and Loring, S. (2017),. JMP start statistics: a guide to statistics and data analysis using JMP. Sas Institute, Cary, State of North Carolina, U.S.A.

Sellke, T., Bayarri, M.J. and Berger, J.O. (2001), "Calibration of ρ values for testing precise null hypotheses", *The American Statistician*, **55**(1), 62-71. https://doi.org/10.1198/000313001300339950.

Shea, H.R. (2009), "Radiation sensitivity of microelectromechanical system devices", *J. Micro/Nanolithography, MEMS and MOEMS*, **8**(3), 031303-031303. https://doi.org/10.1117/1.3152362.

Sjöberg, L. (2004), "Local acceptance of a high-level nuclear waste repository", *Risk Anal. J.*, **24**(3), 737-749. https://doi.org/10.1111/j.0272-4332.2004.00472.x.

SKB (2010), Choice of method–evaluation of strategies and systems for disposal of spent nuclear fuel.

Trevisanello, L., Meneghini, M., Mura, G., Vanzi, M., Pavesi, M., Meneghesso, G. and Zanoni, E. (2008), "Accelerated life test of high brightness light emitting diodes", *IEEE T. Device Mater. Reliab.*, **8**(2), 304-311. http://doi.org/10.1109/TDMR.2008.919596.

Wlodkowski, P.A. (1999), "Physics of failure modes in accelerometers utilizing single crystal piezoelectric materials", Doctoral Dissertation. University of Maryland, College Park, State of Maryland, U.S.A.

Woo, J.T. (2018). "A study on the regulation of durability standard of underground structures monitoring sensors", *J. Korean Tunn. Undergr. Sp. Assoc.*, **20**(1), 73-81. https://doi.org/10.9711/KTAJ.2018.20.1.073.

Zheng, L., Rutqvist, J., Birkholzer, J.T. and Liu, H.H. (2015), "On the impact of temperatures up to 200 C in clay repositories with bentonite engineer barrier systems: A study with coupled thermal, hydrological, chemical, and mechanical modeling", *Eng. Geol.*, **197**, 278-295. https://doi.org/10.1016/j.enggeo.2015.08.026.